HHS Public Access

Author manuscript

Cell Rep. Author manuscript; available in PMC 2017 March 08.

Published in final edited form as:

Cell Rep. 2016 May 17; 15(7): 1430–1441. doi:10.1016/j.celrep.2016.04.035.

Confinement Sensing and Signal Optimization via Piezo1/PKA and Myosin II Pathways

Wei-Chien Hung[1,2,7], **Jessica R. Yang**[3,7], **Christopher L. Yankaskas**[1], **Bin Sheng Wong**[1], **Pei-Hsun Wu**[1,2], **Carlos Pardo-Pastor**[6], **Selma A. Serra**[6], **Meng-Jung Chiang**[3], **Zhizhan Gu**[1], **Denis Wirtz**[1,2,5], **Miguel A. Valverde**[6], **Joy T. Yang**[4,*], **Jin Zhang**[3,*], and **Konstantinos Konstantopoulos**[1,2,5,*]

[1]Department of Chemical and Biomolecular Engineering, Johns Hopkins University, Baltimore, MD 21218, USA

[2]Institute for NanoBioTechnology, Johns Hopkins University, Baltimore, MD 21218, USA

[3]Department of Pharmacology and Molecular Sciences, The Johns Hopkins University School of Medicine, Baltimore, MD 21205, USA

[4]Department of Cell Biology, The Johns Hopkins University School of Medicine, Baltimore, MD 21205, USA

[5]Department of Oncology, The Johns Hopkins University School of Medicine, Baltimore, MD 21205, USA

[6]Laboratory of Molecular Physiology and Channelopathies, Department of Experimental and Health Sciences, Universitat Pompeu Fabra, Carrera del Doctor Aiguader 88, Barcelona 08003, Spain

SUMMARY

Cells adopt distinct signaling pathways to optimize cell locomotion in different physical microenvironments. However, the underlying mechanism that enables cells to sense and respond to physical confinement is unknown. Using microfabricated devices and substrate-printing methods along with FRET-based biosensors, we report that, as cells transition from unconfined to confined spaces, intracellular Ca^{2+} level is increased, leading to phosphodiesterase 1 (PDE1)-dependent suppression of PKA activity. This Ca^{2+} elevation requires Piezo1, a stretch-activated cation channel. Moreover, differential regulation of PKA and cell stiffness in unconfined versus confined cells is abrogated by dual, but not individual, inhibition of Piezo1 and myosin II, indicating that these proteins can independently mediate confinement sensing. Signals activated by Piezo1 and

*Correspondence: jyang@jhmi.edu (J.T.Y.), jzhang32@ucsd.edu (J.Z.), konstant@jhu.edu (K.K.).

[7]Co-first author

SUPPLEMENTAL INFORMATION

Supplemental Information includes Supplemental Experimental Procedures, seven figures, one table, and four movies and can be found with this article online at http://dx.doi.org/10.1016/j.celrep.2016.04.035.

AUTHOR CONTRIBUTIONS

W.-C.H., J.R.Y., J.T.Y., J.Z., and K.K. designed the study. W.-C.H., J.R.Y., C.L.Y., B.S.W., P.-H.W., C.P.-P., S.A.S., and M.-J.C. performed experiments. W.-C.H., J.R.Y., C.L.Y., B.S.W., P.-H.W., C.P.-P., S.A.S., M.-J.C., Z.G., D.W., M.A.V., J.T.Y., J.Z., and K.K. analyzed data. W.-C.H., J.R.Y., J.T.Y., J.Z., and K.K. wrote the paper.

myosin II in response to confinement both feed into a signaling circuit that optimizes cell motility. This study provides a mechanism by which confinement-induced signaling enables cells to sense and adapt to different physical microenvironments.

In Brief

Hung et al. demonstrate that a Piezo1-dependent intracellular calcium increase negatively regulates protein kinase A (PKA) as cells transit from unconfined to confined spaces. The Piezo1/PKA and myosin II signaling modules constitute two confinement-sensing mechanisms. This study provides a paradigm by which signaling enables cells to sense and adapt to different microenvironments.

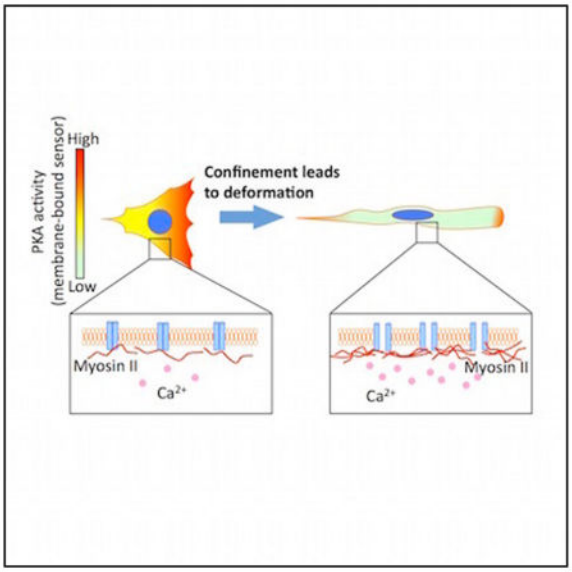

INTRODUCTION

Cells optimize their migratory potential by altering migration modes as they encounter different physical microenvironments (Liu et al., 2015). Cells migrating in a mesenchymal mode share the typical hallmarks of 2D planar migration, including actin-based membrane protrusion, integrin-dependent adhesion, and myosin II-mediated retraction. Alternatively, cells can migrate in other modes when squeezing through channel-like tracks formed between collagen bundles (Liu et al., 2015) or crawl along 1D linear collagen fibers (Doyle et al., 2009). Using microfabricated devices and substrate-printing methods that mimic earmarks of the channel- and fiber-like tracks encountered in vivo, researchers have identified several key mechanisms that are crucial for cell motility under confinement and distinct from those used for locomotion on unconfined 2D substratum (Balzer et al., 2012; Doyle et al., 2009; Harada et al., 2014; Jacobelli et al., 2010; Stroka et al., 2014). One of the mechanisms involves the RhoA/myosin II signaling axis (Beadle et al., 2008; Hung et al., 2013; Jacobelli et al., 2010; Liu et al., 2015). In contrast to Rac1-dependent migration of many cell types on unconfined 2D surfaces, confined migration does not require Rac1-mediated protrusive activities, but instead depends on myosin II-driven contractility (Hung

et al., 2013; Liu et al., 2015). The contractile forces generated by an actomyosin network propel cell locomotion under physical confinement via several strategies (Liu et al., 2015; Petrie et al., 2012, 2014; Tozluoğlu et al., 2013). For efficient migration, cells tune the signaling input in different ways to achieve a balance between Rac1 and RhoA/myosin II, which leads to a strong Rac1 output by unconfined cells and a strong myosin II output by confined cells (Hung et al., 2013). One unresolved question is how do cells differentially regulate Rac1 and RhoA/myosin II in response to different degrees of confinement.

Using an α4 integrin-expressing CHO cell model (referred to as CHO-α4WT cells) that recapitulates aspects of the motile activities of invasive melanoma cells, we have reported that CHO-α4WT cells respond to physical confinement by tuning Rac1 and RhoA/myosin II activities to optimize cell motility (Hung et al., 2013). Intriguingly, the Rac1 activity in CHO-α4WT cells is tightly regulated by cyclic AMP (cAMP)-dependent protein kinase A (PKA), which phosphorylates the α4 integrin cytoplasmic tail (Han et al., 2003). PKA, a regulator of a wide array of physiological functions (Howe, 2011), is also known to play an important role in the migration of carcinoma cells and in the regulation of RhoA and Rac1 functions in several cooperative pathways (Newell-Litwa and Horwitz, 2011). Therefore, we hypothesized that PKA could play the central role in tuning the complex networking of RhoA/Rac1 in response to mechanical cues.

Another important unresolved question is: What is the underlying mechanosensing mechanism that allows the cells to respond to physical confinement? Mechanotransduction involves mechanisms by which external force directly induces conformational change or activation of a mechanosensor. Several mechanisms have been proposed which involve three major classes of mechanosensors: (1) stretch-activated ion channels, (2) elements of the cytoskeleton and nuclear matrix, and (3) components of adhesion complexes and extracellular matrix.

Like many stretch-activated cationic channels, Piezo1 (also named Fam38A) (Coste et al., 2010) serves as a mechanosensor that tightly regulates cell development, proliferation, and survival by allowing calcium influx in response to different types of external forces (Eisenhoffer et al., 2012; Li et al., 2014). In addition, prior studies have reported that calcium influx plays an important role of regulating cAMP/PKA activity, which in turn modulates the phosphorylation level of downstream molecules (Howe, 2011; Lee et al., 1999). To investigate the interplay between PKA and confinement-induced mechanosensing mechanisms, we employed well-established Förster resonance energy transfer (FRET)-based PKA activity and calcium reporters in conjunction with microfabrication and substrate printing technologies to explore the real-time modulation of PKA activity, and its interaction with relevant signaling molecules in response to physical confinement. We also examined changes in cell mechanics in response to confinement using atomic force microscopy.

We demonstrate that efficient cell migration in confined spaces is achieved by complex feedback interactions between Piezo1/Ca^{2+}/PDE1/PKA and myosin/Rac1 pathways. We also provide evidence for Piezo1- and myosin II-mediated confinement-sensing mechanisms. These findings provide a mechanism by which cells adapt to different degrees of physical confinement and optimize their motile activities.

RESULTS

Differential Modulation of PKA Activity Is Required for Optimized Migration of CHO-α4WT Cells through Unconfined versus Confined Spaces

We have reported that α4β1 integrin, ectopically expressed in CHO cells (CHO-α4WT), promotes cell migration through both unconfined and confined spaces (Hung et al., 2013). Efficient CHO-α4WT cell locomotion in different physical microenvironments requires the differential modulation of the binding between α4 integrin and paxillin such that the binding occurs preferentially in confined, but not in unconfined cells (Hung et al., 2013). α4/paxillin binding forms a ternary complex with GIT1 that inhibits Rac activation (Nishiya et al., 2005). Due to signaling crosstalk between Rac1 and myosin II, the differential regulation of α4/paxillin binding leads to an optimized signaling output that favors Rac1 activation in unconfined cells versus myosin II-driven contractility in confined cells (Hung et al., 2013). α4/paxillin binding is negatively regulated via PKA-dependent phosphorylation of α4 integrin at Ser988 (Han et al., 2003). In view of these observations, we hypothesize that PKA is differentially modulated in unconfined versus confined cells. Specifically, we postulate that physical confinement suppresses PKA activity, which in turn results in decreased α4Ser988 phosphorylation, thereby leading to optimized cell migration in confined spaces.

We employed two distinct assays to test our hypothesis and compare cell motility in unconfined versus confined microenvironments. In the first assay, cells were induced to migrate toward a chemotactic source through fibronectin-coated microchannels of fixed height (10 μm) and length (200 μm), but varying widths (50, 20, 10, 6, or 3 μm) (Figure S1A). In this microchannel assay, cells in wide channels (20 μm or wider) are unconfined, whereas those in narrow channels (6 μm or narrower) are confined (Hung et al., 2013). The second assay compares the motility of cells plated on 8 μm-wide 1D fibronectin-printed lines (referred to as 1D printed lines hereafter) versus unconfined 2D fibronectin-coated surfaces. This assay examines cell response to lateral confinement resulting from adhesion/spreading constraints (Figure S1D). Although the two assays are distinct, CHO-α4WT cells inside narrow channels and on 1D printed lines assume an elongated morphology and require myosin IIA for efficient migration (Doyle et al., 2009; Hung et al., 2013).

To test our hypothesis, we first demonstrated that phosphorylation of α4Ser988 was indeed suppressed in CHO-α4WT cells when confined either in narrow channels or on 1D printed lines compared to those in wide channels or on 2D surfaces, respectively (Figure S1). We then examined the effects of a PKA activator, forskolin, and a PKA inhibitor, Rp-cAMPs, on cell migration as a function of the degree of physical confinement, using our microchannel assay. CHO-α4WT cells treated with forskolin (50 μM) migrated as efficiently as vehicle controls in wide (50 or 20 μm) channels, but displayed a markedly reduced velocity in narrow (10, 6, or 3 μm) channels (Figures 1A and 1B; Movie S1). In contrast to forskolin, PKA inhibition using Rp-cAMPs (50 μM) had the opposite effect; cells migrated efficiently in narrow channels, but with significantly lower velocity relative to vehicle control in wide channels (Figures 1A and 1B; Movie S1). We next tested the effects of PKA modulation on CHO-α4WT cells migrating on 1D printed lines. In accord with our microchannel data,

induction of PKA activity using forskolin (50 μM) suppressed both the velocity and instantaneous speed of cells migrating on 1D printed lines (Figures 1C–1E; Movie S2). On the other hand, inhibition of PKA activity using Rp-cAMP enhanced 1D cell migration (Figures 1C–1E; Movie S2). Taken together, low PKA activity is required for optimal migration of CHO-α4WT cells in confined spaces, whereas high PKA activity is necessary for efficient cell migration in unconfined microenvironments. We propose that cells are capable of tuning the level of PKA activity in response to different degrees of physical confinement.

Physical Confinement Suppresses Membrane-Associated PKA Activity

To test the hypothesis that PKA activity is differentially regulated in unconfined versus confined spaces, we utilized a FRET-based PKA activity biosensor, AKAR4, to measure PKA activity levels in unconfined and confined CHO-α4WT cells. PKA activity is detected as an increase in FRET ratio (yellow-to-cyan emission ratio upon excitation of CFP) due to PKA phosphorylation-induced conformational change of the sensor. To assess plasma membrane-localized PKA activity, we used a plasma membrane-targeted version of AKAR4, AKAR4-Kras (Depry et al., 2011) (Figure 2A). AKAR4-Kras was transiently transfected into CHO-α4WT cells, and the initial FRET ratio prior to drug treatments was obtained to quantify the basal levels of membrane-associated PKA activity (referred to as PKA activity hereafter). Confined cells exhibited lower initial FRET ratio compared to unconfined cells (Figures 2B and 2E), indicating that confined cells had lower basal PKA activity than unconfined cells. As controls, we first showed that the FRET ratio did not significantly correlate with transfection efficiency (Figure S2A). Moreover, AKAR4-Kras, but not a kinase activity-insensitive version of the biosensor, TA-Kras, detected an increase in PKA activity when the cells were treated with both forskolin and the phosphodiesterase inhibitor 3-isobutyl-1-methylxanthine IBMX to stimulate PKA activity (Figure S2B). In contrast to AKAR4-Kras, TA-Kras did not generate a differential FRET ratio in unconfined versus confined cells (Figure S2C), indicating that the differential FRET ratios observed in unconfined versus confined cells are indeed due to differences in PKA activities rather than changes in cell shape.

To substantiate the reduction of PKA activity observed in confined cells, we quantified the effects of the PKA inhibitor H89 (10 μM) in unconfined and confined CHO-α4WT cells. A smaller reduction of FRET ratio is indicative of a lower basal PKA activity. Indeed, after 30 min of cell treatment with H89, unconfined cells exhibited a pronounced reduction (20.6% ± 4.2%) in FRET ratio, whereas only a modest decrease (7.0% ± 1.2%) was detected in confined cells (Figures 2B and 2C). Similar data were obtained using Rp-cAMP to inhibit PKA activity (Figure S2D). Taken together, these data indicate that confined CHO-α4WT cells possess lower basal PKA activity levels than unconfined cells. Along these lines, a decrease in PKA activity levels is observed as cells transit from an unconfined 2D surface to a narrow (3 μm in width) channel (Figure 2D; Movie S3). In addition, PKA activity was significantly lower in cells plated on 1D printed lines than those plated on 2D surfaces (Figure S3A).

Integrins have been reported to play important roles in the spatiotemporal regulation of PKA in order to stimulate CHO cell migration on 2D substrates (Lim et al., 2007). We thus investigated if the reduced PKA activity in confinement is mediated by α4 and/or α5 integrins. To this end, we quantified the basal PKA activity levels in three cell lines: CHO-α4WT that expresses both α4 and α5 integrins, parental CHO that only expresses α5 integrin, and CHO-B2 that lacks α4 and α5 integrins (Chen et al., 2012; Schreiner et al., 1989). Interestingly, physical confinement significantly suppressed PKA activity in all three cell lines (Figure 2E), suggesting that α4 and α5 integrins are not required for the differential levels of PKA activity in unconfined versus confined cells. However, it is noteworthy that the expression of α4 and α5 integrins elevates the basal levels of PKA activity in both unconfined and confined cells. Collectively, these results indicate that although α4 and α5 integrins enhance the overall PKA activity, they are not required for the cells to sense and respond to physical confinement.

Elevated Intracellular Calcium in Confined Cells Negatively Regulates PKA via Piezo1 and PDE1

In light of prior work showing the role of calcium in cell migration and the presence of negative crosstalk between calcium and PKA (Howe, 2011; Lee et al., 1999), we hypothesize that the changes in PKA activity induced by physical confinement are regulated via Ca^{2+}-dependent signaling mechanisms. To test this, we used a FRET-based Ca^{2+} indicator, Yellow Cameleon 3.6 (YC 3.6) (Nagai et al., 2004) to monitor intracellular Ca^{2+} levels in both unconfined and confined CHO-α4WT cells (Figure 3A). Upon Ca^{2+} binding, the CaM-M13 molecular switch undergoes a conformational change, thereby resulting in a FRET ratio increase. Confined CHO-α4WT cells exhibited higher basal Ca^{2+} levels than unconfined cells (Figures 3B and 3C). Moreover, an increase in intracellular calcium levels was also observed as cells transit from a 2D surface to a narrow (3 μm in width) channel (Figure 3D; Movie S4) or plated on 1D printed lines compared to those on 2D surfaces (Figure S3B). To investigate the potential source of higher basal Ca^{2+} levels in confined cells, we treated CHO-α4WT with the stretch-activated cation channel inhibitor GsMTx4 (Suchyna et al., 2000). This treatment suppressed the Ca^{2+} levels in confined cells down to those of un-confined cells (Figure 3C). Moreover, GsMTx4 failed to alter the Ca^{2+} levels in unconfined cells (Figure 3C). Because it has been reported that GsMTx4 most effectively blocks a stretch-activated cation channel, Piezo1 (Bae et al., 2011; Li et al., 2014), we transiently knocked down Piezo1 in CHO-α4WT cells. Immunoblotting showed that the Piezo1 level was significantly reduced in Piezo1 small interfering (si)RNA transfected cells. The efficacy of Piezo1 siRNA was further confirmed by showing that transfected cells displayed an altered morphology (e.g., larger spreading area and tail elongation) consistent with that reported in the literature (Li et al., 2014) (Figure 3E). Similar to the GsMTx4 treatment, knock down of Piezo1 abolished the confinement-induced elevation of the intracellular Ca^{2+} level (Figure 3F). Moreover, Piezo1-knockdown cells migrated slower in narrow (3 μm), but not wide (50 μm), channels and required longer times to enter the narrow channels compared to scramble control cells (Figure 3G). Taken together, these data suggest that physical confinement elevates intracellular Ca^{2+} via the stretch-activated ion channel Piezo1.

To directly access the effect of Ca^{2+} on PKA, we measured PKA activity in CHO-α4WT cells transfected with AKAR4-Kras in the presence or absence of a Ca^{2+} chelator BAPTA-AM (40 μM). An increase in PKA activity was detected in confined cells following BAPTA treatment (Figure 4A). This response is attributed to the higher intracellular calcium levels in untreated confined cells, which negatively regulate PKA activity. On the other hand, no significant change was noted in unconfined cells under BAPTA treatment (Figure 4A), which is consistent with their low basal intracellular calcium levels. To delineate the mechanism underlying Ca^{2+}-mediated suppression of PKA activity in confined cells, we investigated the potential contribution of phosphodiesterases (PDEs), which are enzymes that downregulate PKA by hydrolyzing cAMP. As a first step, cells transfected with AKAR4-Kras were treated with the general PDE inhibitor IBMX (100 μM) (Herbst et al., 2011). Both unconfined and confined cells treated with IBMX displayed an increase in PKA activity (Figure 4B), thereby demonstrating the presence of basal PDE activity in CHO-α4WT cells and the inhibitory effect of PDEs on PKA. Notably, a significant difference in the amplitude of the AKAR4-Kras response was observed between unconfined and confined cells following treatment with IBMX (Figures 4A and 4B). The larger increase in PKA activity in confined cells in response to IBMX indicates that confined cells exhibit higher PDE activity than unconfined cells, which contributes to their differential basal PKA activity levels.

Next, we wished to identify the PDE responsible for regulating Ca^{2+}-mediated suppression of PKA activity in confined cells. Certain PDEs, such as PDE1 and PDE4, are specifically upregulated by Ca^{2+} (Mika et al., 2015; Sonnenburg et al., 1995). PDE1 is regulated by Ca^{2+}/calmodulin through direct interactions, whereas PDE4 is regulated through a phosphorylation-dependent activation by Ca^{2+}/calmodulin-dependent protein kinase II (CaMKII) (Mika et al., 2015). Cell treatment with the PDE4-specific inhibitor rolipram (10 μM) elicited a similar increase in PKA activity in both unconfined and confined cells (Figure 4C). These results indicate that, although PDE4 contributes to the suppression of basal PKA activity, it does not exert a differential effect in response to physical confinement. In contrast, cell treatment with a PDE1-selective inhibitor 8 methoxy methyl IBMX (8MM-IBMX, 100 μM) caused a pronounced increase in PKA activity levels in confined cells, whereas only a modest increase was noted in unconfined cells (Figures 4C and 4D). These data indicate that PDE1 contributes to the confinement-dependent PKA suppression. As a control, we inhibited a non-Ca^{2+}-dependent PDE, PDE3, with milrinone (1 μM) and monitored the FRET response from AKAR4-Kras. As predicted, there was no detectable enhancement in PKA activity in either unconfined or confined cells, indicating that PDE3 is not involved in regulating PKA activity in response to changes in intracellular Ca^{2+} and physical confinement (Figure 4C). Importantly, knocking down Piezo1, similar to PDE1 inhibition, induced a higher PKA activity increase in confined relative to unconfined spaces (Figure 4E).

Taken together, our data provide clear evidence that the differential PKA regulation in response to confinement is Ca^{2+}-dependent and proceeds mainly through the Piezo1/Ca^{2+}/PDE1 pathway.

Inhibition of Piezo1 and Myosin II Synergistically Abrogates Confinement-Induced PKA Suppression

Our finding that Piezo1 is required for confinement-dependent elevation of intracellular Ca^{2+} suggests that this stretch-activated channel may mediate confinement sensing. We reasoned that, if Piezo1 is the sole confinement-sensing mediator, then inhibition of Piezo1 should abrogate the differential PKA activity in unconfined versus confined cells. However, knocking down Piezo1 in CHO-α4WT cells suppressed, but failed to abolish the confinement-induced differential PKA activity (Figure 4F). Likewise, the confinement-induced differential PKA activity persisted when the cells were treated with the PDE1 inhibitor (Figure 4D). These data suggest that cells can sense confinement via an alternative pathway independent of Piezo1/PDE1.

External forces have been reported to induce assembly of myosin II bi-polar filaments and actomyosin bundles (Fernandez-Gonzalez et al., 2009; Ren et al., 2009). This force-sensitive activity of myosin II led us to hypothesize that myosin II may also mediate confinement sensing, thereby leading to a cascade of signaling events that ultimately suppress PKA. To test this possibility, we treated CHO-α4WT cells with the myosin inhibitor blebbistatin (50 μM). This treatment caused a significant increase in PKA activity of both unconfined and confined CHO-α4WT and parental CHO cells relative to vehicle control (Figures 5A–5B′). Rac1 is known to activate A-kinase anchoring proteins (AKAPs) that in turn recruit and activate PKA at the leading edge of migrating cells (Westphal et al., 2000; Yamashita et al., 2011). Due to the multiple interactions between Rac1- and myosin II-related pathways, myosin II may negatively regulate PKA activity via a Rac1-dependent pathway. To test this possibility, CHO cells were treated concurrently with blebbistatin and the Rac1 inhibitor NSC23766 (20 μM). This dual treatment abolished the enhancing effect of blebbistatin on the PKA activity of both un-confined and confined cells (Figures 5B and 5C), thereby indicating that myosin II downregulates PKA activity through a Rac1-dependent pathway. However, treating the cells with blebbistatin alone or with blebbistatin and the Rac1 inhibitor NSC23766 failed to abolish the difference in the PKA activity of unconfined versus confined cells (Figure 5C), indicating that the myosin II/Rac1 pathway is dispensable for confinement-induced PKA suppression. Notably, treatment of Piezo1-knockdown cells with blebbistatin effectively abrogated the confinement-induced suppression of PKA activity in both CHO-α4WT and parental CHO Cells (Figure 5D). Similar observations were made after cell treatment with both blebbistatin and the PDE1 inhibitor (Figure S4). These findings reveal the potential existence of two confinement-sensing pathways: one mediated by Piezo1 via PDE1 and the other by myosin II. Each of these confinement-sensing mediators can act independently in the absence of the other.

Inhibition of Piezo1 and Myosin II Synergistically Abrogates Confinement-Induced Enhancement of Cell Stiffness

Because stretch-activated cation channels are activated by increased membrane tension, we evaluated the ability of cells to resist deformation (referred to as cell stiffness) in response to confinement imposed by 1D printed lines versus unconfined cells on 2D surfaces. Specifically, we employed atomic force microscopy to measure the elastic modulus by indenting a cell with an atomic force microscopy (AFM) cantilever tip. The applied force

was calculated from the degree of bending (deflection) of the cantilever as a function of indentation position of the AFM tip, using the Sneddon/Hertz model (Thomas et al., 2013) (Figures 6A and 6B).

First, we investigated the effects of various pharmacological inhibitors on cell stiffness. On both 2D surfaces and 1D printed lines, blebbistatin, 8MM-IBMX, or GsMTx4 treatment reduced cell stiffness (Figure 6C), whereas inhibition of PKA using Rp-cAMPs or its activation with forskolin enhanced or diminished cell stiffness, respectively (Figure 6D). These results indicate that cell stiffness can be influenced by stretch-activated cation channels/PDE1/PKA and myosin II pathways regardless the microenvironments, possibly involving PKA-dependent regulation of myosin II (Figures S5A–S5D).

Next, we compared the stiffness of the cells on 1D printed lines versus 2D surfaces. The cells on 8 μm-wide 1D printed lines displayed markedly higher stiffness compared to cells on a 2D surface (controls in Figures 6C and 6D) or on 15 μm- and 40 μm-wide lines (Figure S4F). Notably, the differential cell stiffness between 2D and 1D persisted under individual pharmacological (Figures 6C and 6D) or siRNA (Figure 6E) treatments. Therefore, perturbing PKA, PDE1, myosin II, or Piezo1 alone did not abolish confinement-induced enhancement of cell stiffness on 1D compared to 2D. Remarkably, dual disruption of myosin II and Piezo1 or PDE1 effectively abrogated the difference in cell stiffness between 1D and 2D (Figures 6E and S4E). These data further support the existence of two independent confinement-sensing mechanisms mediated by Piezo1/PDE1 and myosin II, respectively. Furthermore, the difference in cell stiffness between 1D and 2D was abolished by latrunculin treatment, indicating that both confinement-sensing mechanisms depend on the actin cytoskeleton (Figure S5F).

Piezo1/Ca^{2+}/PDE1/PKA Pathway Contributes to Confined Migration of Invasive Melanoma Cells

In order to investigate the role of the Piezo1/Ca^{2+}/PDE1/PKA pathway in regulating confined migration of cancer cells, we tested an invasive melanoma cancer cell line A375-SM. We have previously shown that A375-SM cells optimize their motile activities in unconfined and confined spaces by modulating Rac1 and myosin II signaling outputs in the same manner as CHO-α4WT cells (Hung et al., 2013). According to the literature (Okamoto et al., 2005) and the GEO2R database, A375 cells express relatively high levels of Piezo1 compared to other stretch-activated cation channels. Using RT-quantitative (q) PCR, we confirmed that A375-SM cells indeed express higher levels of Piezo1 than Piezo2 and other putative stretch-activated cation channels sensitive to GsMTx-4, including TRPC1 (Maroto et al., 2005) and TRPC6 (Spassova et al., 2006) (Figure 7A). Functional expression of GsMTx4-sensitive Piezo channels in A375-SM cells was confirmed by recording whole-cell currents while cells were mechanically stimulated with a glass probe (Figure S6A). Confinement by narrow channels or 1D printed lines concurrently suppressed PKA activity and increased intracellular Ca^{2+} in A375-SM cells (Figures 7B–7D, S6B, and S6C). Similar to our findings with CHO-α4WT cells (Figure 1A), migration of A375-SM cells in narrow (3 μm) channels was markedly repressed by forskolin, but enhanced by Rp-cAMP (Figure 7E). Moreover, the stretch-activated cation channel inhibitor GsMTx4 and the PDE1

inhibitor 8MM-IBMX significantly suppressed confined migration, but not unconfined migration (Figure 7F). Consistent with the pharmacological inhibitor data, depletion of Piezo1 or PDE1 reduced only the confined migration of A375-SM cells (Figure 7G). Although blebbistatin alone also suppressed the confined migration of A375 and CHO-α4WT cells, no additional suppression was noted upon simultaneous disruption of Piezo1 and myosin II activity (Figure 7G; Table S1). These data are consistent with the notion that myosin II acts downstream of the Piezo1/Ca^{2+}/PDE1/PKA pathway to promote confined cell migration (Figure S7).

To better mimic the in vivo 3D microenvironment, we next tested the migration of A375-SM cells in a 3D collagen gel (Figure 7H). In concert with our microchannel data, forskolin-treated or Piezo1-knockdown A375-SM cells migrated at a slower velocity than control cells (Figures 7I and 7J). Collectively, these data illustrate the critical roles of Piezo1 and PKA in cell migration through physiologically relevant microenvironments.

DISCUSSION

Combining FRET-based biosensors with microfabrication techniques and AFM, we demonstrate that confinement induces an elevation of intracellular calcium level, and this response requires Piezo1, a stretch-activated cation channel. The elevated calcium in turn suppresses PKA activity near the plasma membrane, via a PDE1-dependent pathway. This pathway provides a mechanism by which cells sense and respond to physical confinement. Moreover, we provide evidence that myosin II also contributes to confinement sensing. We further show that confinement-induced changes in PKA activity and cell stiffness are completely abrogated by dual, but not individual, treatment of cells with Piezo1-RNAi and blebbistatin, indicating that Piezo1 and myosin II can independently mediate confinement sensing.

Piezo1 belongs to a family of stretch-activated channels (SACs) (Coste et al., 2010). It has been reported that SACs facilitate Ca^{2+} influx in response to tension at the plasma membrane of bacteria (Sukharev et al., 1994), specialized eukaryotic sensory cells (Meyers et al., 2003), and skeletal muscle cells (Yeung et al., 2005). Here, we report that Piezo1 also functions as mechanosensor for regulating cell migration under confinement. When cells move in narrow microchannels or on 1D printed lines, they are physically confined and forced to elongate. This elongation may stretch the lipid bilayer and the cortical actomyosin network, thus generating tension at the plasma membrane, leading to activation of Piezo1. Besides Piezo1 activation, the interplay among confinement, cell elongation, and cell mechanics may also induce cortical tension and force-sensitive assembly of myosin II bi-polar filaments (Fernandez-Gonzalez et al., 2009; Ren et al., 2009). Alternatively, the cortical tension may activate other cytoskeletal mechanosensors (Sawada et al., 2006) that in turn activate myosin II. Having two independent sensing machineries mediated by Piezo1 and myosin II may enhance the sensitivity of cells to confinement and broaden the range of confinement signals to be sensed. Moreover, because myosin II also acts as a downstream effector directly contributing to migratory activities, it may “short-cut” the mechanotransduction circuit and fasten cell responses to confinement.

It is known that integrins play a pivotal role in mechanosensing (Charras and Sahai, 2014). However, we show that α4 and α5 integrins are dispensable for cells to sense confinement and suppress PKA activity. In addition, synergy and compensation are not observed between α4 integrin and either PDE1 or myosin II. These observations are consistent with the notion that in confined microenvironments integrin-mediated cell adhesion becomes less important for cell motility (Balzer et al., 2012; Bergert et al., 2015) and confined migration is favored by low adhesion (Bergert et al., 2015; Liu et al., 2015; Raman et al., 2013). We show that, although not contributing to confinement sensing, α4 integrins do participate in PKA regulation in a confinement-independent manner, which supports the AKAP function of α4 integrins as reported in the literature (Lim et al., 2007).

In view of our data and those in the literature, we propose a model in which confinement signals sensed by two independent pathways, the Piezo1 and myosin II pathways, are integrated through a complex feedback circuit, resulting in optimal circuit activity for efficient cell migration (Figure S7). One of the circuits involves a double negative feedback loop between PKA and myosin II. In CHO-α4WT cells, confinement-induced suppression of PKA leads to decreased PKA-dependent phosphorylation of α4 integrin at Ser988. Inhibition of α4Ser988 phosphorylation promotes the formation of an α4/paxillin/GIT1 ternary complex that blocks Rac1, thus enhancing myosin II activity (Hung et al., 2013; Nishiya et al., 2005). PKA may also regulate Rac1 and myosin II via α4 integrin-independent pathways in which RhoA or Rho-GEF is directly phosphorylated and inhibited by PKA (Diviani et al., 2004; Tkachenko et al., 2011). Therefore, confinement-induced PKA suppression leads to enhanced myosin II activity via α4 integrin-dependent and -independent pathways. Our data indicate that, myosin II acts not only as a downstream PKA effector, but also as an upstream regulator that suppresses PKA activity. The suppression depends on Rac1. Several Rac1 effectors, including WAVE1 and WAVE2, function as AKAPs that recruit and activate PKA at the cell cortex proximal to the plasma membrane (Westphal et al., 2000; Yamashita et al., 2011). Therefore, the activity of membrane-associated PKA could be affected by inhibition of the Rac1/WAVEs pathways. Thus, PKA and myosin II/Rac1 form a double negative feedback loop. Another circuit activity involves a positive feedback between Piezo1/calcium and myosin II. Calcium can directly enhance myosin II via calmodulin-mediated pathways (Wolenski, 1995) or via a G protein-mediated pathway (Somlyo and Somlyo, 2003). On the other hand, myosin II-driven contractility plays a key role in activation of stretch-activated ion channels (Sbrana et al., 2008). The presence of these feedback loops may allow the circuit system to respond to physical confinement with ultrasensitivity and even exhibit switch-like behaviors. As a consequence, small changes in the physical environment may flip the PKA-Myosin II switch, leading to a new balance between Myosin II and Rac1 activities, thereby optimizing the efficiency of cell motility. The combined feedback mechanisms provide a strategy for signal optimization.

We used cell stiffness as a readout for confinement-induced cell responses. Our data reveal that cell stiffness can be regulated by myosin II-dependent and myosin II-independent pathways, and both of these pathways depend on actin filaments. A potential myosin II-independent mechanism involves calcium-induced changes in the cortical actin network. Altered dynamics and arrangements of actin filaments could increase cortical tension

without an involvement of myosin II-driven contractility (Carvalho et al., 2013; Janmey et al., 1990).

Knock down of Piezo1 results in larger cell spreading area and tail elongation (Figure 3E) reminiscent to myosin IIA-depleted CHO-α4WT cells (Hung et al., 2013), consistent with the role of myosin IIA in the Piezo1-dependent pathway. It is noteworthy that myosin IIB-knockdown bone marrow-derived mesenchymal cells display cell morphology (Raab et al., 2012) similar to that of MIIA-depleted CHO-α4WT cells. The role of different myosin II isoforms in confinement sensing of different cell types is worth further investigating.

In summary, we propose a model in which physical confinement is sensed by Piezo1/Ca^{2+}/PDE1/PKA- and myosin II-dependent pathways through a complex feedback circuit, resulting in the regulation of cell locomotion. Tuning of this circuit is also necessary for the efficient migration of invasive A375-SM melanoma cells in different physical microenvironments including narrow channels and physiologically relevant 3D collagen gels. Therefore, the mechanotransduction signaling mechanism uncovered in this work could be a more general mechanism for cells to sense and adapt to microenvironments with different degrees of physical confinement and optimize their motile activities.

EXPERIMENTAL PROCEDURES

siRNA Experiments

In transient knockdown experiments, PDE1 siRNA (Santa Cruz for CHO cells and OriGene for A375-SM cells) and Piezo1 siRNA (Santa Cruz for CHO cells and Life technology for A375-SM cells) were used. Transient transfection was performed using Lipofectamine 2000.

Microchannel Assay

A polydimethylsiloxane (PDMS)-based microchannel device was fabricated as previously described (Balzer et al., 2012; Hung et al., 2013; Tong et al., 2012). Channels were coated with fibronectin (20 μg/ml).

PKA Activity and Intracellular Calcium Imaging

Cells transfected with biosensors, AKAR4-Kras, TA-Kras, or Yellow Cameleon, were imaged every 10–30 s and analyzed as previously described (Depry et al., 2011).

Stiffness Measurement

An atomic force microscope (MFP-1D; Asylum Research) (Hanley et al., 2004; Raman et al., 2011) was used to measure cell stiffness. The cantilever height was adjusted such that each approach cycle generated a slight force (~1–2 nN) onto the cell surface before reproach. Reproach velocity was 25 μm/s. Stiffness was analyzed and quantified as previously described (Thomas et al., 2013) using the Sneddon/Hertz model of indentation force to calculate the elastic modulus (i.e., the stiffness) of the cell.

Tracking Cells Embedded in 3D Collagen I Matrix

A375-SM cells were embedded in 1 mg/ml type-I collagen gels and tracked as described previously (Fraley et al., 2010).

Statistical Analysis

Data are expressed as mean ± SEM. Statistical significance of differences between means was determined by Student's t test or one-way ANOVA followed by the Tukey test for multiple comparisons, where appropriate.

Supplementary Material

Refer to Web version on PubMed Central for supplementary material.

Acknowledgments

The research is supported by awards from the NIH (R01 DK073368 and DP1 CA174423 to J.Z. and R01 CA183804 and R01 GM114675 to K.K.); Kleberg Foundation and American Heart Association (to K.K.); Spanish Ministry of Economy and Competitiveness (SAF2012-38140 and SAF2015-69762-R); Fondo de Investigación Sanitaria (RD12/0042/0014); and FEDER Funds (to M.A.V.).

References

Bae C, Sachs F, Gottlieb PA. The mechanosensitive ion channel Piezo1 is inhibited by the peptide GsMTx4. Biochemistry. 2011; 50:6295–6300. [PubMed: 21696149]

Balzer EM, Tong Z, Paul CD, Hung WC, Stroka KM, Boggs AE, Martin SS, Konstantopoulos K. Physical confinement alters tumor cell adhesion and migration phenotypes. FASEB J. 2012; 26:4045–4056. [PubMed: 22707566]

Beadle C, Assanah MC, Monzo P, Vallee R, Rosenfeld SS, Canoll P. The role of myosin II in glioma invasion of the brain. Mol Biol Cell. 2008; 19:3357–3368. [PubMed: 18495866]

Bergert M, Erzberger A, Desai RA, Aspalter IM, Oates AC, Charras G, Salbreux G, Paluch EK. Force transmission during adhesion-independent migration. Nat Cell Biol. 2015; 17:524–529. [PubMed: 25774834]

Carvalho K, Lemière J, Faqir F, Manzi J, Blanchoin L, Plastino J, Betz T, Sykes C. Actin polymerization or myosin contraction: two ways to build up cortical tension for symmetry breaking. Philos Trans R Soc Lond B Biol Sci. 2013; 368:20130005. [PubMed: 24062578]

Charras G, Sahai E. Physical influences of the extracellular environment on cell migration. Nat Rev Mol Cell Biol. 2014; 15:813–824. [PubMed: 25355506]

Chen L, Vicente-Manzanares M, Potvin-Trottier L, Wiseman PW, Horwitz AR. The integrinligand interaction regulates adhesion and migration through a molecular clutch. PLoS ONE. 2012; 7:e40202. [PubMed: 22792239]

Coste B, Mathur J, Schmidt M, Earley TJ, Ranade S, Petrus MJ, Dubin AE, Patapoutian A. Piezo1 and Piezo2 are essential components of distinct mechanically activated cation channels. Science. 2010; 330:55–60. [PubMed: 20813920]

Depry C, Allen MD, Zhang J. Visualization of PKA activity in plasma membrane microdomains. Mol Biosyst. 2011; 7:52–58. [PubMed: 20838685]

Diviani D, Abuin L, Cotecchia S, Pansier L. Anchoring of both PKA and 14-3-3 inhibits the Rho-GEF activity of the AKAP-Lbc signaling complex. EMBO J. 2004; 23:2811–2820. [PubMed: 15229649]

Doyle AD, Wang FW, Matsumoto K, Yamada KM. One-dimensional topography underlies three-dimensional fibrillar cell migration. J Cell Biol. 2009; 184:481–490. [PubMed: 19221195]

Eisenhoffer GT, Loftus PD, Yoshigi M, Otsuna H, Chien CB, Morcos PA, Rosenblatt J. Crowding induces live cell extrusion to maintain homeostatic cell numbers in epithelia. Nature. 2012; 484:546–549. [PubMed: 22504183]

Fernandez-Gonzalez R, de Simoes SM, Röper JC, Eaton S, Zallen JA. Myosin II dynamics are regulated by tension in intercalating cells. Dev Cell. 2009; 17:736–743. [PubMed: 19879198]

Fraley SI, Feng Y, Krishnamurthy R, Kim DH, Celedon A, Longmore GD, Wirtz D. A distinctive role for focal adhesion proteins in three-dimensional cell motility. Nat Cell Biol. 2010; 12:598–604. [PubMed: 20473295]

Han J, Rose DM, Woodside DG, Goldfinger LE, Ginsberg MH. Integrin alpha 4 beta 1-dependent T cell migration requires both phosphorylation and dephosphorylation of the alpha 4 cytoplasmic domain to regulate the reversible binding of paxillin. J Biol Chem. 2003; 278:34845–34853. [PubMed: 12837751]

Hanley WD, Wirtz D, Konstantopoulos K. Distinct kinetic and mechanical properties govern selectin-leukocyte interactions. J Cell Sci. 2004; 117:2503–2511. [PubMed: 15159451]

Harada T, Swift J, Irianto J, Shin JW, Spinler KR, Athirasala A, Diegmiller R, Dingal PC, Ivanovska IL, Discher DE. Nuclear lamin stiffness is a barrier to 3D migration, but softness can limit survival. J Cell Biol. 2014; 204:669–682. [PubMed: 24567359]

Herbst KJ, Allen MD, Zhang J. Spatiotemporally regulated protein kinase A activity is a critical regulator of growth factor-stimulated extra-cellular signal-regulated kinase signaling in PC12 cells. Mol Cell Biol. 2011; 31:4063–4075. [PubMed: 21807900]

Howe AK. Cross-talk between calcium and protein kinase A in the regulation of cell migration. Curr Opin Cell Biol. 2011; 23:554–561. [PubMed: 21665456]

Hung WC, Chen SH, Paul CD, Stroka KM, Lo YC, Yang JT, Konstantopoulos K. Distinct signaling mechanisms regulate migration in unconfined versus confined spaces. J Cell Biol. 2013; 202:807–824. [PubMed: 23979717]

Jacobelli J, Friedman RS, Conti MA, Lennon-Dumenil AM, Piel M, Sorensen CM, Adelstein RS, Krummel MF. Confinement-optimized three-dimensional T cell amoeboid motility is modulated via myosin IIA-regulated adhesions. Nat Immunol. 2010; 11:953–961. [PubMed: 20835229]

Janmey PA, Hvidt S, Lamb J, Stossel TP. Resemblance of actin-binding protein/actin gels to covalently crosslinked networks. Nature. 1990; 345:89–92. [PubMed: 2158633]

Lee J, Ishihara A, Oxford G, Johnson B, Jacobson K. Regulation of cell movement is mediated by stretch-activated calcium channels. Nature. 1999; 400:382–386. [PubMed: 10432119]

Li J, Hou B, Tumova S, Muraki K, Bruns A, Ludlow MJ, Sedo A, Hyman AJ, McKeown L, Young RS, et al. Piezo1 integration of vascular architecture with physiological force. Nature. 2014; 515:279–282. [PubMed: 25119035]

Lim CJ, Han J, Yousefi N, Ma Y, Amieux PS, McKnight GS, Taylor SS, Ginsberg MH. Alpha4 integrins are type I cAMP-dependent protein kinase-anchoring proteins. Nat Cell Biol. 2007; 9:415–421. [PubMed: 17369818]

Liu YJ, Le Berre M, Lautenschlaeger F, Maiuri P, Callan-Jones A, Heuzé M, Takaki T, Voituriez R, Piel M. Confinement and low adhesion induce fast amoeboid migration of slow mesenchymal cells. Cell. 2015; 160:659–672. [PubMed: 25679760]

Maroto R, Raso A, Wood TG, Kurosky A, Martinac B, Hamill OP. TRPC1 forms the stretch-activated cation channel in vertebrate cells. Nat Cell Biol. 2005; 7:179–185. [PubMed: 15665854]

Meyers JR, MacDonald RB, Duggan A, Lenzi D, Standaert DG, Corwin JT, Corey DP. Lighting up the senses: FM1-43 loading of sensory cells through nonselective ion channels. J Neurosci. 2003; 23:4054–4065. [PubMed: 12764092]

Mika D, Richter W, Conti M. A CaMKII/PDE4D negative feedback regulates cAMP signaling. Proc Natl Acad Sci USA. 2015; 112:2023–2028. [PubMed: 25646485]

Nagai T, Yamada S, Tominaga T, Ichikawa M, Miyawaki A. Expanded dynamic range of fluorescent indicators for Ca(2+) by circularly permuted yellow fluorescent proteins. Proc Natl Acad Sci USA. 2004; 101:10554–10559. [PubMed: 15247428]

Newell-Litwa KA, Horwitz AR. Cell migration: PKA and RhoA set the pace. Curr Biol. 2011; 21:R596–R598. [PubMed: 21820627]

Nishiya N, Kiosses WB, Han J, Ginsberg MH. An alpha4 integrin-paxillin-Arf-GAP complex restricts Rac activation to the leading edge of migrating cells. Nat Cell Biol. 2005; 7:343–352. [PubMed: 15793570]

Okamoto I, Pirker C, Bilban M, Berger W, Losert D, Marosi C, Haas OA, Wolff K, Pehamberger H. Seven novel and stable translocations associated with oncogenic gene expression in malignant melanoma. Neoplasia. 2005; 7:303–311. [PubMed: 15967107]

Petrie RJ, Gavara N, Chadwick RS, Yamada KM. Nonpolarized signaling reveals two distinct modes of 3D cell migration. J Cell Biol. 2012; 197:439–455. [PubMed: 22547408]

Petrie RJ, Koo H, Yamada KM. Generation of compartmentalized pressure by a nuclear piston governs cell motility in a 3D matrix. Science. 2014; 345:1062–1065. [PubMed: 25170155]

Raab M, Swift J, Dingal PC, Shah P, Shin JW, Discher DE. Crawling from soft to stiff matrix polarizes the cytoskeleton and phosphoregulates myosin-II heavy chain. J Cell Biol. 2012; 199:669–683. [PubMed: 23128239]

Raman PS, Alves CS, Wirtz D, Konstantopoulos K. Single-molecule binding of CD44 to fibrin versus P-selectin predicts their distinct shear-dependent interactions in cancer. J Cell Sci. 2011; 124:1903–1910. [PubMed: 21558419]

Raman PS, Paul CD, Stroka KM, Konstantopoulos K. Probing cell traction forces in confined microenvironments. Lab Chip. 2013; 13:4599–4607. [PubMed: 24100608]

Ren Y, Effler JC, Norstrom M, Luo T, Firtel RA, Iglesias PA, Rock RS, Robinson DN. Mechanosensing through cooperative interactions between myosin II and the actin crosslinker cortexillin I. Curr Biol. 2009; 19:1421–1428. [PubMed: 19646871]

Sawada Y, Tamada M, Dubin-Thaler BJ, Cherniavskaya O, Sakai R, Tanaka S, Sheetz MP. Force sensing by mechanical extension of the Src family kinase substrate p130Cas. Cell. 2006; 127:1015–1026. [PubMed: 17129785]

Sbrana F, Sassoli C, Meacci E, Nosi D, Squecco R, Paternostro F, Tiribilli B, Zecchi-Orlandini S, Francini F, Formigli L. Role for stress fiber contraction in surface tension development and stretch-activated channel regulation in C2C12 myoblasts. Am J Physiol Cell Physiol. 2008; 295:C160–C172. [PubMed: 18480300]

Schreiner CL, Bauer JS, Danilov YN, Hussein S, Sczekan MM, Juliano RL. Isolation and characterization of Chinese hamster ovary cell variants deficient in the expression of fibronectin receptor. J Cell Biol. 1989; 109:3157–3167. [PubMed: 2531750]

Somlyo AP, Somlyo AV. Ca2+ sensitivity of smooth muscle and nonmuscle myosin II: modulated by G proteins, kinases, and myosin phosphatase. Physiol Rev. 2003; 83:1325–1358. [PubMed: 14506307]

Sonnenburg WK, Seger D, Kwak KS, Huang J, Charbonneau H, Beavo JA. Identification of inhibitory and calmodulin-binding domains of the PDE1A1 and PDE1A2 calmodulin-stimulated cyclic nucleotide phosphodiesterases. J Biol Chem. 1995; 270:30989–31000. [PubMed: 8537356]

Spassova MA, Hewavitharana T, Xu W, Soboloff J, Gill DL. A common mechanism underlies stretch activation and receptor activation of TRPC6 channels. Proc Natl Acad Sci USA. 2006; 103:16586–16591. [PubMed: 17056714]

Stroka KM, Jiang H, Chen SH, Tong Z, Wirtz D, Sun SX, Konstantopoulos K. Water permeation drives tumor cell migration in confined microenvironments. Cell. 2014; 157:611–623. [PubMed: 24726433]

Suchyna TM, Johnson JH, Hamer K, Leykam JF, Gage DA, Clemo HF, Baumgarten CM, Sachs F. Identification of a peptide toxin from Grammostola spatulata spider venom that blocks cation-selective stretch-activated channels. J Gen Physiol. 2000; 115:583–598. [PubMed: 10779316]

Sukharev SI, Blount P, Martinac B, Blattner FR, Kung C. A large-conductance mechanosensitive channel in E. coli encoded by mscL alone. Nature. 1994; 368:265–268. [PubMed: 7511799]

Thomas G, Burnham NA, Camesano TA, Wen Q. Measuring the Mechanical Properties of Living Cells Using Atomic Force Microscopy (Jove-J Vis Exp). 2013

Tkachenko E, Sabouri-Ghomi M, Pertz O, Kim C, Gutierrez E, Machacek M, Groisman A, Danuser G, Ginsberg MH. Protein kinase A governs a RhoA-RhoGDI protrusion-retraction pacemaker in migrating cells. Nat Cell Biol. 2011; 13:660–667. [PubMed: 21572420]

Tong Z, Balzer EM, Dallas MR, Hung WC, Stebe KJ, Konstantopoulos K. Chemotaxis of cell populations through confined spaces at single-cell resolution. PLoS ONE. 2012; 7:e29211. [PubMed: 22279529]

Tozluoğlu M, Tournier AL, Jenkins RP, Hooper S, Bates PA, Sahai E. Matrix geometry determines optimal cancer cell migration strategy and modulates response to interventions. Nat Cell Biol. 2013; 15:751–762. [PubMed: 23792690]

Westphal RS, Soderling SH, Alto NM, Langeberg LK, Scott JD. Scar/WAVE-1, a Wiskott-Aldrich syndrome protein, assembles an actin-associated multi-kinase scaffold. EMBO J. 2000; 19:4589–4600. [PubMed: 10970852]

Wolenski JS. Regulation of calmodulin-binding myosins. Trends Cell Biol. 1995; 5:310–316. [PubMed: 14732095]

Yamashita H, Ueda K, Kioka N. WAVE2 forms a complex with PKA and is involved in PKA enhancement of membrane protrusions. J Biol Chem. 2011; 286:3907–3914. [PubMed: 21119216]

Yeung EW, Whitehead NP, Suchyna TM, Gottlieb PA, Sachs F, Allen DG. Effects of stretch-activated channel blockers on [Ca2+]i and muscle damage in the mdx mouse. J Physiol. 2005; 562:367–380. [PubMed: 15528244]

Highlights

- Calcium is elevated via Piezo1 as cells transit from unconfined to confined spaces
- PKA activity is suppressed in confined relative to unconfined spaces
- Piezo1-dependent calcium increase negatively regulates PKA via PDE1 in confinement
- Piezo1/PDE1/PKA and myosin II independently mediate confinement sensing

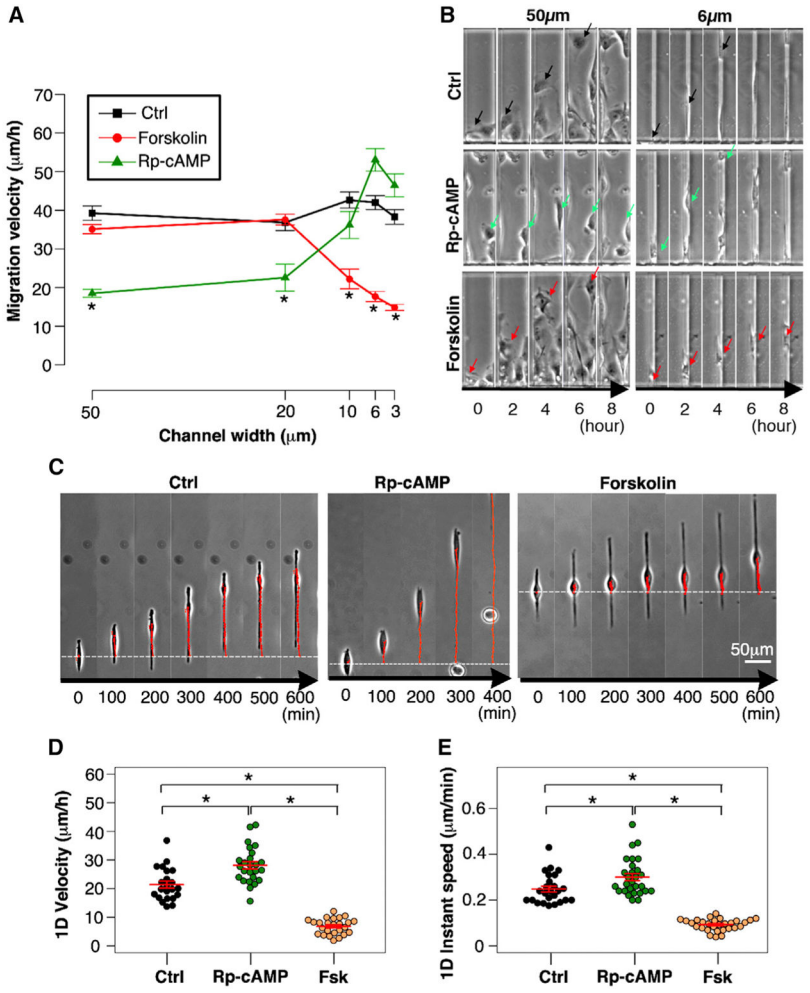

Figure 1. Modulation of PKA Activity Has Differential Effects on Unconfined versus Confined Cell Migration

(A–E) CHO-α4WT cells were treated with either the PKA activator forskolin or the PKA inhibitor Rp-cAMP or appropriate vehicle control and allowed to migrate inside fibronectin-coated micro-channels (A and B) or on 8 μm-wide 1D printed lines (C–E). Their migration velocities (A and D) and instantaneous speeds (E) were quantified. The time-lapse images of migrating cells in designated channel widths (B) and 1D printed lines (C) are shown. The data represent the mean ± SEM (*$p < 0.05$). See also Figure S1 and Movies S1 and S2.

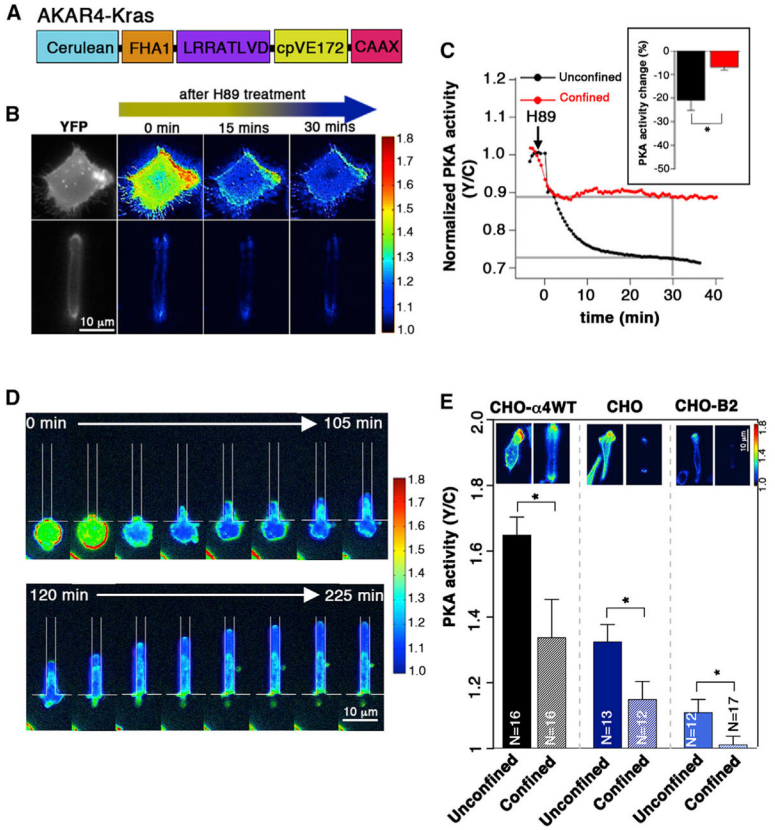

Figure 2. Confinement Suppresses PKA Activity

(A) Schematic diagram of AKAR4-Kras biosensor. The biosensor is composed of a substrate peptide, cpVE172, and the phosphoamino-binding domain (FHA1), each tagged with a fluorescent protein and the membrane targeting motif CAAX.

(B) CHO-α4WT cells expressing AKAR4-Kras were plated on unconfined spaces or induced to migrate into 3 μm channels to experience confinement. Yellow fluorescent protein (YFP) and FRET ratiometric images of confined and unconfined cells before the PKA inhibitor H89 was added (0 min) and at 15 and 30 min after the addition.

(C) Representative curves of normalized PKA activity of CHO-α4WT cells in confined or unconfined spaces after addition of H89. The bar graph represents the percentage of decay of PKA activity at 30 min after the addition of H89.

(D) Time-lapse FRET ratiometric images of a CHO-α4WT cell expressing AKAR4-KRAS, as the cell is migrating from an unconfined area into a 3 μm channel.

(E) The basal PKA activities of confined and un-confined CHO-α4WT, CHO, and CHO-B2 cells. The data in the bar graphs in (C) and (E) represent the mean ± SEM (*$p < 0.05$).

See also Figure S2 and Movie S3.

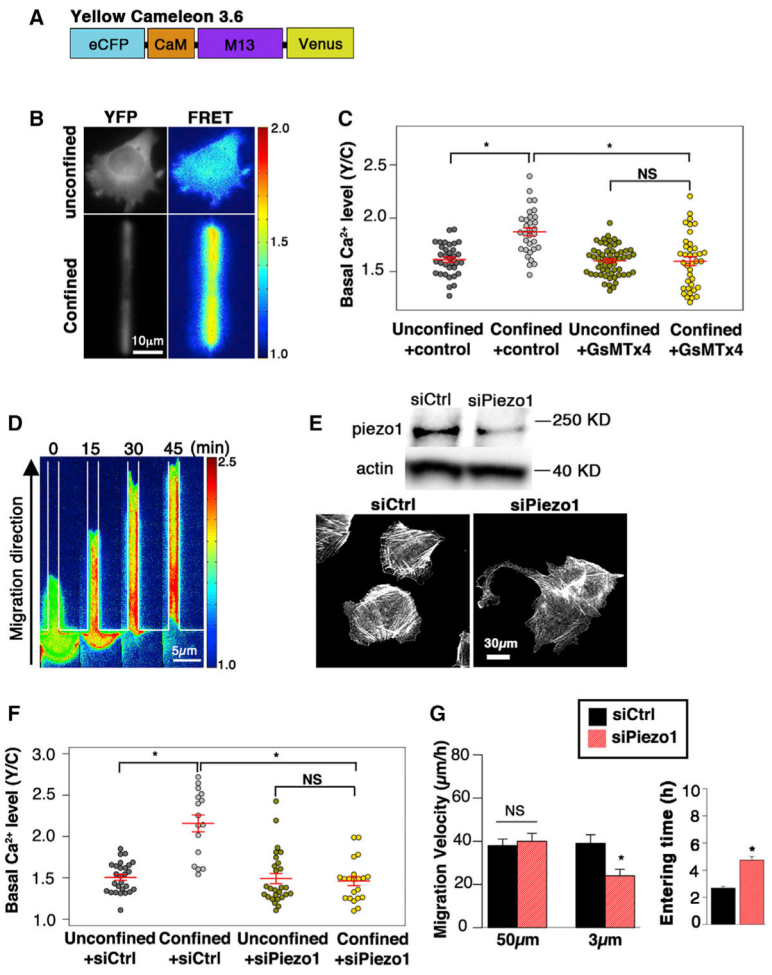

Figure 3. Piezo1 Regulates Intracellular Calcium in Response to Confinement

(A) Schematic diagram of FRET-based calcium indicator YC3.6.

(B) YFP and FRET ratiometric images of unconfined and confined CHO-α4WT cells expressing YC3.6.

(C) The basal calcium levels of unconfined or confined CHO-α4WT cells, treated with either the stretch-activated ion channel inhibitor GsMTx4 (10 μM) or vehicle control, were quantified by measuring the initial FRET (i.e., yellow-to-cyan ratio).

(D) Time-lapse FRET ratiometric images of a CHO-α4WT cell expressing YC3.6, as the cell is migrating from an unconfined area into a 3 μm channel.

(E) CHO-α4WT cells were either transfected with a siRNA for Piezo1 (siPiezo1) or a control siRNA (siCtrl). The depletion of Piezo1 by siRNA was demonstrated by immunoblotting using an anti-Piezo1 antibody. The actin was stained by phalloidin in siCtrl and siPiezo1 transfected cells to display morphological changes.

(F) The basal calcium levels of unconfined or confined CHO-α4WT cells transfected with either siPiezo or siCtlr were quantified by measuring the initial FRET (i.e., yellow-to-cyan ratio).

(G) CHO-α4WT cells were transfected with Piezo1 siRNA, or Control siRNA, and induced to migrate inside fibronectin-coated microchannels of 50 μm or 3 μm in width. The

migration velocities and entering time through a 3 μm channel of more than 30 cells were analyzed from three independent experiments. The data represent the mean ± SEM (*$p < 0.05$).

See also Movie S4.

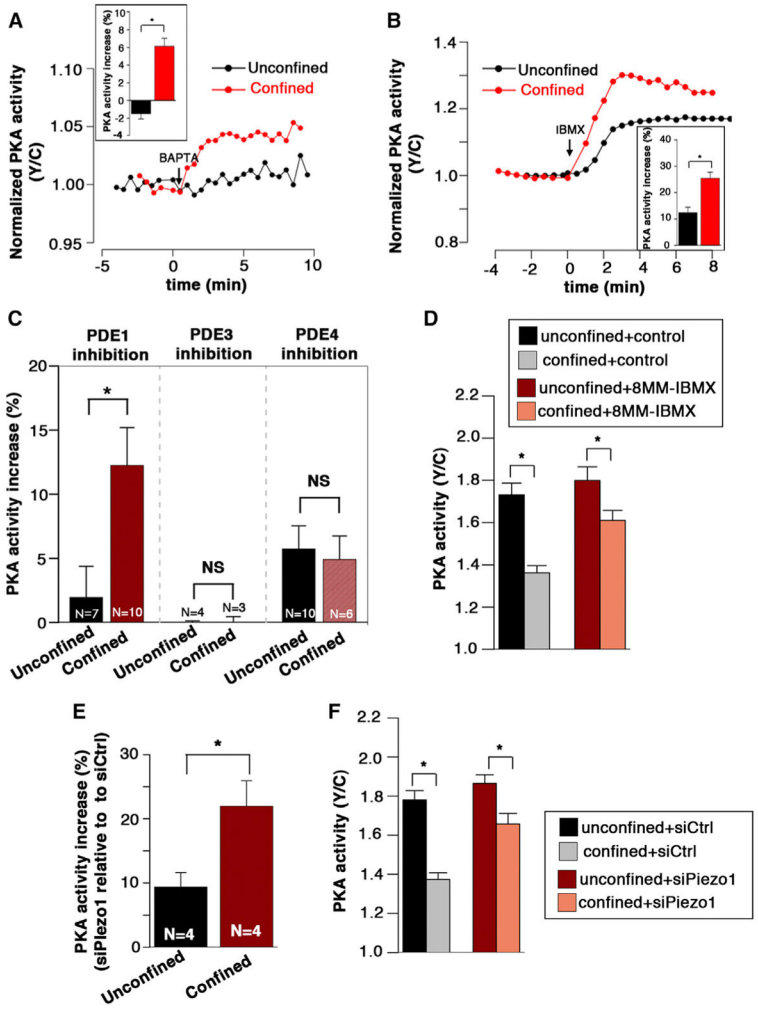

Figure 4. Calcium Modulates PKA Activity via a Piezo1/PDE1 Pathway

(A) Representative curves of normalized PKA activity in unconfined (n = 7) and confined (n = 5) CHO-α4WT cells expressing AKAR4-KRAS, treated with BAPTA at time 0 min. The corresponding bar graph shows the increase of PKA activity after 5 min of drug treatment.

(B) Representative curves of normalized PKA activity in unconfined and confined CHO-α4WT cells expressing AKAR4-KRAS before and after IBMX addition. The corresponding bar graph shows the increase of PKA activity after 5 min of drug treatment.

(C) Changes in PKA activity in unconfined and confined CHO-α4WT cells after treatment with PDE1, PDE3, and PDE4 inhibitors, respectively. (D) The basal PKA activity of unconfined and confined CHO-α4WT cells treated with vehicle control or the PDE1 inhibitor 8MM-IBMX.

(E) Changes in PKA activity in unconfined and confined CHO-α4WT cells transfected with either Piezo1 siRNA (siPiezo) or control siRNA (siCtrl). Four independent experiments were performed. Averaged PKA activity of more than ten cells for each siRNA condition was determined in each independent experiment in order to calculate percent increase.

(F) The basal PKA activity of unconfined and confined CHO-α4WT cells transfected with siPiezo1 or siCtrl. The data represent the mean ± SEM. For (D) and (F), n > 40 cells were included in each condition (*p < 0.05).

See also Figure S3.

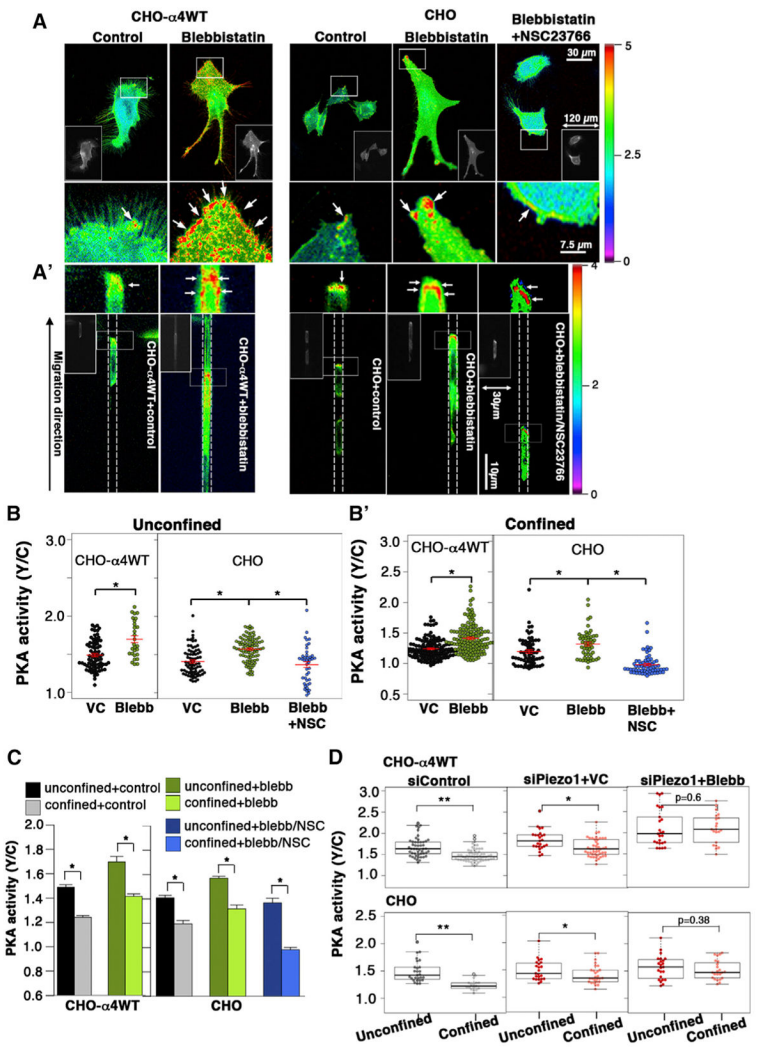

Figure 5. Myosin II- and Piezo1-Dependent Mechanosensing Contribute to Confinement-Induced PKA Suppression

(A and A′) Unconfined (A) and confined (A′) CHO-α4WT and CHO cells expressing AKAR4-Kras were treated with blebbistatin or vehicle control. The arrows indicate the high PKA activity at the leading edge of cells.

(B and B′) The PKA activities in unconfined (B) and confined (B′) CHO-α4WT and CHO cells with each designated drug treatment where quantified and graphed.

(C) CHO-α4WT or CHO cells treated with vehicle control were compared with cells under designated drug treatments in order to determine the effect of the drugs on confinement-induced suppression of PKA activity.

(D) CHO-α4WT or CHO cells were transfected with control siRNA (siCtrl) or Piezo1 siRNA (siPiezo1). The siPiezo1-transfected cells were treated with blebbistatin or with vehicle control. The basal PKA activities of the cells under these treatments were quantified and presented as integrated dot/box plots for comparing the effects of the treatments on confinement-induced PKA suppression. The data represent the mean ± SEM (*$p < 0.05$ and ** < 0.0005).

See also Figure S4.

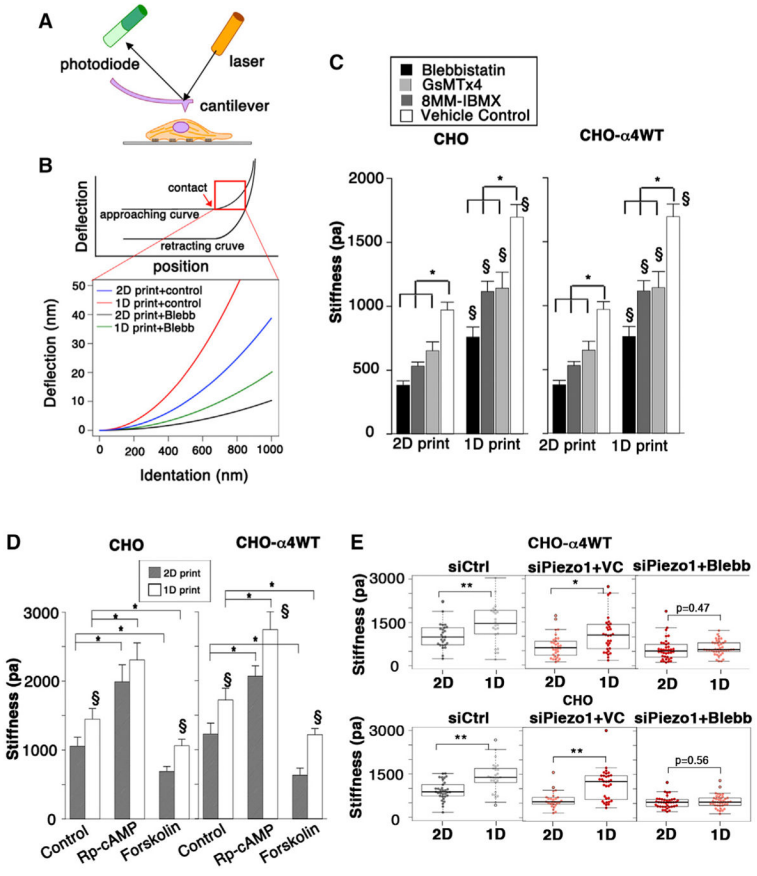

Figure 6. Confinement Enhances Cell Stiffness via Piezo1- and Myosin II-Dependent Mechanosensing

(A) Schematic diagram of AFM technique used for measuring cell stiffness.

(B) Representative approach curves from parental CHO cells cultured on 2D surfaces or 1D printed lines showing deflection (degree bending of AFM cantilever) as a function of indented position.

(C) Bar graphs represent the elastic modulus (stiffness) of parental CHO and CHO-α4WT cells plated on a 2D printed area or 1D printed lines and treated with blebbistatin, GsMTx-4, 8MM-IBMX, or a vehicle control.

(D) Bar graphs represent the elastic modulus (stiffness) of parental CHO and CHO-α4WT cells plated on a 2D printed area or 1D printed lines and treated with Rp-cAMP, forskolin, or a vehicle control. Elastic modulus is calculated from the approach curve. Data represent the mean ± SEM for n > 35 cells for each condition. *p < 0.05. χp < 0.05 for 1D print versus 2D print for each respective condition.

(E) Integrated dot and box plots comparing the effects of the designated interventions on the stiffness of the cells plated on 1D versus 2D fibronectin-printed substrates. CHO-α4WT or CHO cells transfected with either Piezo1 siRNA (siPiezo1) or control siRNA (siCtrl) and treated with blebbistatin or vehicle control were examined. *p < 0.05. **p < 0.0005.

See also Figure S5.

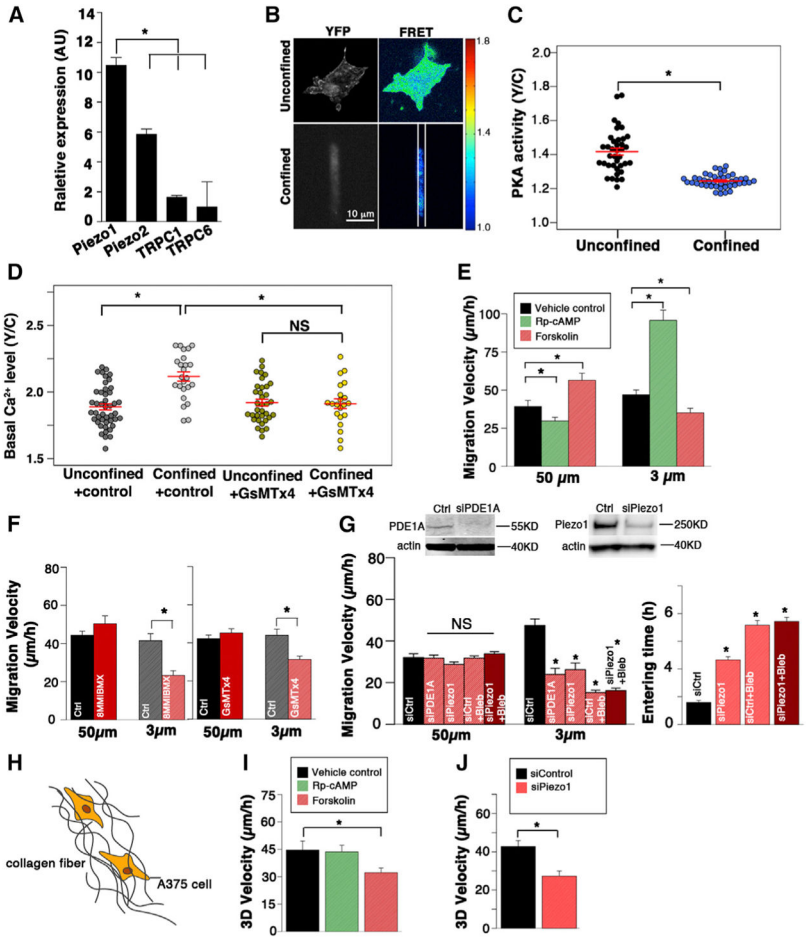

Figure 7. The Piezo1/Ca^{2+}/PDE1/PKA Pathway Regulates Confined Migration of A375-SM

(A) mRNA expression profile of stretch-activated cation channels by qRT-PCR.

(B) YFP and FRET ratiometric images of unconfined and confined A375-SM melanoma cells expressing AKAR4-Kras.

(C) Dot plot comparing the basal PKA activities of unconfined and confined A375-SM cells.

(D) The basal calcium levels of unconfined versus confined A375-SM cells, treated with either the stretch-activated ion channel inhibitor GsMTx4 (10 μM) or vehicle control, were quantified by measuring the initial FRET (i.e., yellow-to-cyan ratio).

(E) A375-SM cells were treated with either the PKA inhibitor Rp-cAMP or the PKA activator forskolin or appropriate vehicle control and induced to migrate inside fibronectin-coated microchannels of 50 μm or 3 μm in width.

(F) A375-SM cells were treated with the PDE1 inhibitor 8MM-IBMX or GsMTx4 or appropriate vehicle control and induced to migrate inside fibronectin-coated microchannels of 50 μm or 3 μm in width.

(G) A375-SM cells were transfected with PDE1 siRNA, Piezo1 siRNA, or control siRNA in the presence or absence of blebbistatin and then induced to migrate inside fibronectin-coated microchannels of 50 μm or 3 μm in width. In (E)–(G), the migration velocity and time required to enter 3 μm channels were determined by analyzing more than 30 cells from three independent experiments.

(H) Schematic of 3D migration of A375-cells in a collagen gel.
(I) 3D migration velocity of A375-SM cells treated with Rp-cAMP, forskolin, or vehicle control.
(J) 3D migration velocity of A375-SM cells transfected with Piezo1 siRNA or Control siRNA. 3D migration velocities were quantified by analyzing more than 100 cells from four independent experiments. The data represent the mean ± SEM (*$p < 0.05$). See also Figures S6 and S7.